CHAPTER IV
RESULTS AND DISCUSSION

4.1 Fresh Catalyst Characterizations

4.1.1 Brunauer-Emmett-Tellet (BET) Surface Area Analysis

Textural properties of the TiO_2 support and Pd/TiO_2 catalysts (surface area, total pore volume, mean pore diameter) were measured by Brunauer-Emmett-Tellet surface area analyzer. From the results in Table 4.1, the surface area of TiO_2 (Degussa P 25) is 50.50 m^2/g which is close to the given property (50 m^2/g). The surface area of prepared catalyst is slightly lower when compared to the TiO_2 support due to the deposition of the metal on the TiO_2 surface.

Table 4.1 Textural properties of the catalysts

Catalyst	Surface area, S_{BET} (m^2/g)	Total pore volume (cm^3/g)	Mean pore diameter (nm)
P25- TiO_2	50.50	0.230	18.50
P25-IWI	48.80	0.228	18.70

4.1.2 Inductively Coupled Plasma Optical Emission Spectrometry (ICP-OES)

The quantity of active metal on catalyst was measured. The result shows that the actual amount of Pd loaded on TiO_2 support is 0.96%. The result reveals that the technique used in catalyst preparation (incipient wetness impregnation, IWI) gives the amount in Pd loading on TiO_2 support closer to expected metal loading amount.

4.1.3 Thermogravimetry and Differential Thermal Analysis (TG/DTA)

Thermogravimetry and differential thermal analysis was used to study the thermal decomposition behavior and the suitable calcination temperature of the catalyst. Figure 4.1 shows TG-DTA curve of 1 wt% Pd/TiO_2 catalyst prepared by

incipient wetness impregnation method. The DTA curve showed two main exothermic regions. The first exothermic peak at temperature lower than 150 °C is contributed to the removal of physisorbed water molecules. The exothermic region between 150 and 500 °C corresponds to the removal of organic remnants and chemisorbed water molecule, respectively (Hague, D.C., and Mayo, M.J., 1994). The TG result reveals that the weight losses completely end at a temperature of approximately 500 °C. Therefore, the appropriate calcination temperature for Pd/TiO_2 catalyst is 500 °C.

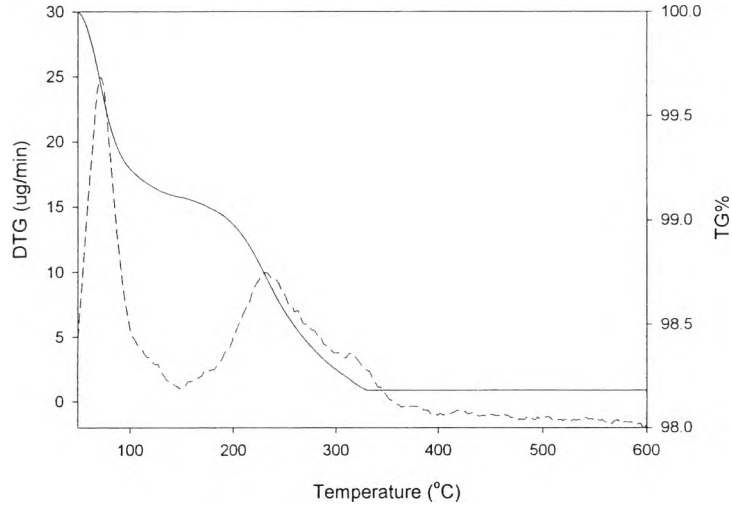

Figure 4.1 TG-DTA profile of 1 wt% Pd/TiO_2 catalyst prepared via incipient wetness impregnation method (IWI).

4.2 Feed Characterization

The production of hydrogenated biodiesel varies depending on the properties of feedstock and the production process. In this work, feedstocks were characterized for their components, fatty acid compositions and their impurities contents by gas chromatograph, AOAC 996.06-GC method and ICP technique, respectively.

4.2.1 Standard Analysis

The chemical standards such as n-dodecane (n-C_{12}), n-pentadecane (n-C_{15}), n-hexadecane (n-C_{16}), n-heptadecane (n-C_{17}), n-octadecane (n-C_{18}), n-eicosane (n-C_{20}), hexadecanol, octadecanol, palmitic acid, oleic acid, stearic acid, ester group, monoglyceride group, diglyceride group, and triglyceride group were analyzed by gas chromatograph equipped with an FID detector (Agilent 7890) to identify peaks of compositions of feedstocks, intermediates and products. The chromatograms are shown in Figure 4.2. The retention time and response factor of the standards are shown in Table 4.2.

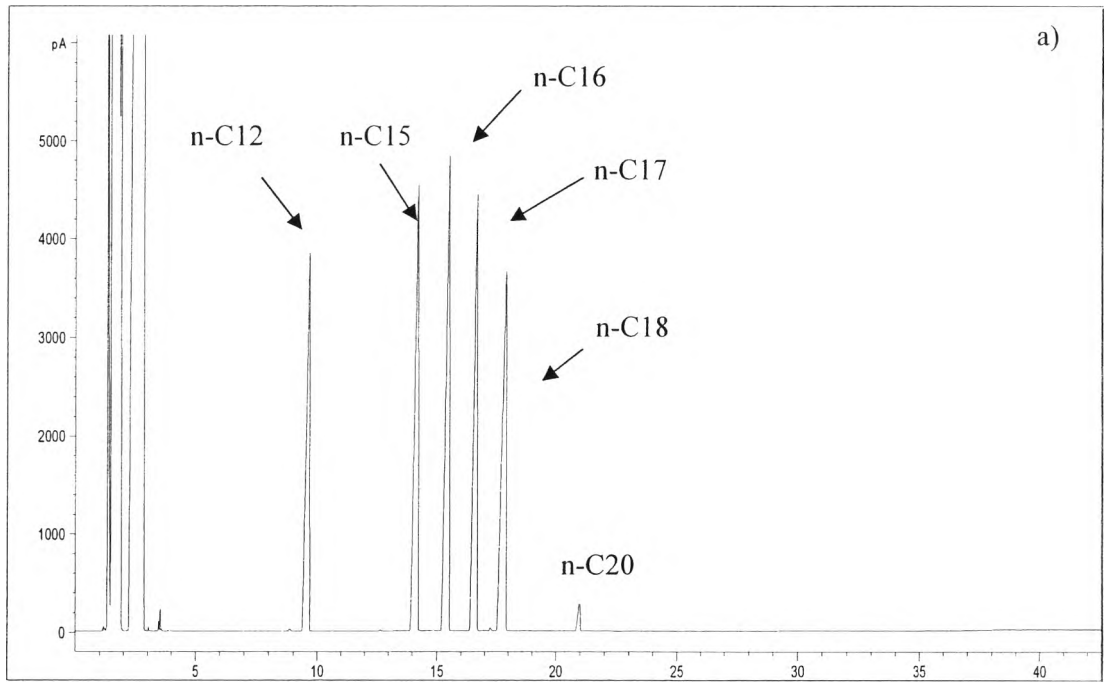

Figure 4.2 Chromatograms of standard chemicals, (a) n-pentadecane, n-hexadecane, n-heptadecane, n-octadecane, (b) hexadecanol, octadecanol, palmitic acid, stearic acid, oleic acid, (c) monopalmitin, (d) stearyl palmitate, palmityl stearate, stearyl stearate, (e) dipalmitin, distearin, and (f) tripalmitin, tristearin.

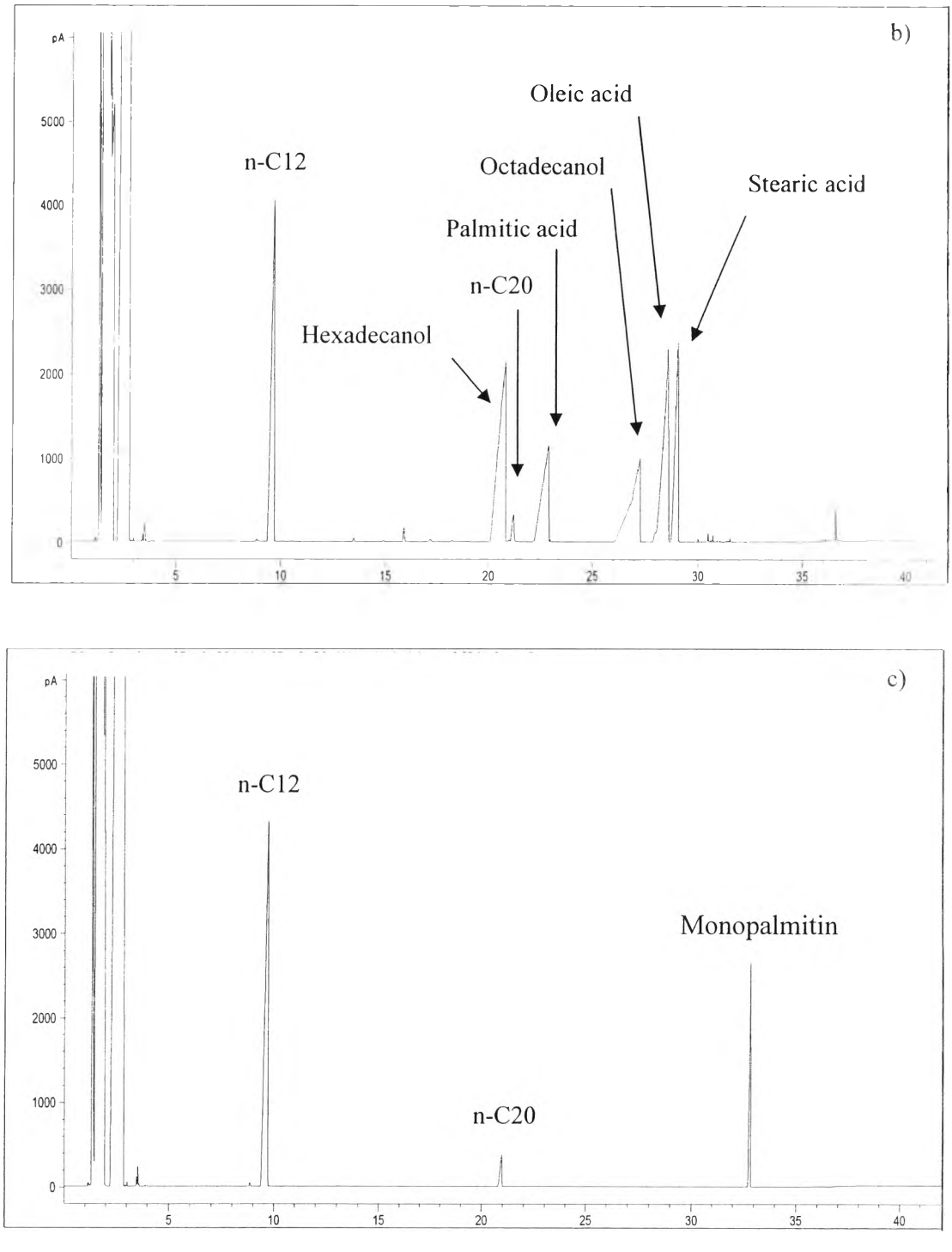

Figure 4.2 (cont.) Chromatograms of standard chemicals, (a) n-pentadecane, n-hexadecane, n-heptadecane, n-octadecane, (b) hexadecanol, octadecanol, palmitic acid, stearic acid, oleic acid, (c) monopalmitin, (d) stearyl palmitate, palmityl stearate, stearyl stearate, (e) dipalmitin, distearin, and (f) tripalmitin, tristearin.

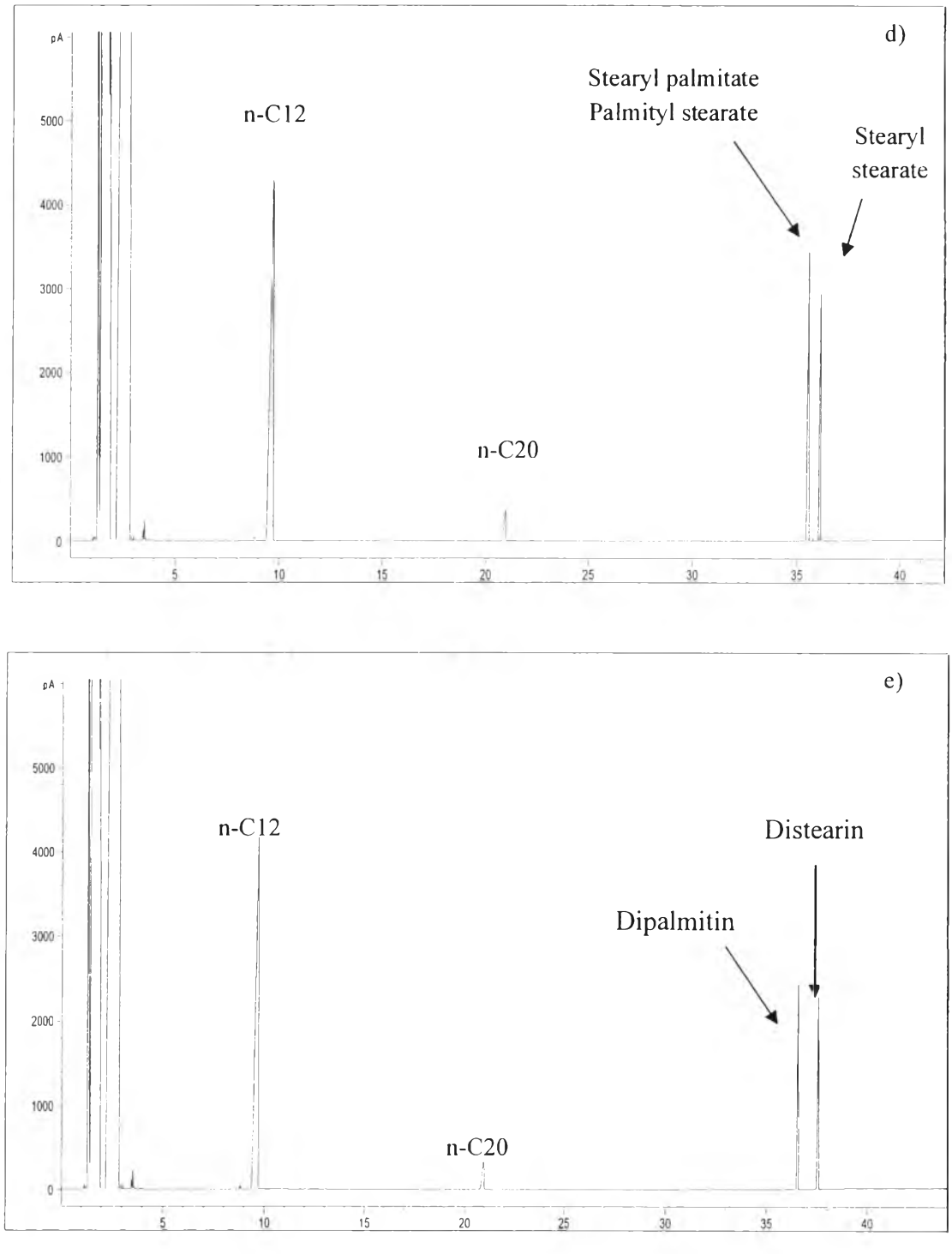

Figure 4.2 (cont.) Chromatograms of standard chemicals, (a) n-pentadecane, n-hexadecane, n-heptadecane, n-octadecane, (b) hexadecanol, octadecanol, palmitic acid, stearic acid, oleic acid, (c) monopalmitin, (d) stearyl palmitate, palmityl stearate, stearyl stearate, (e) dipalmitin, distearin, and (f) tripalmitin, tristearin.

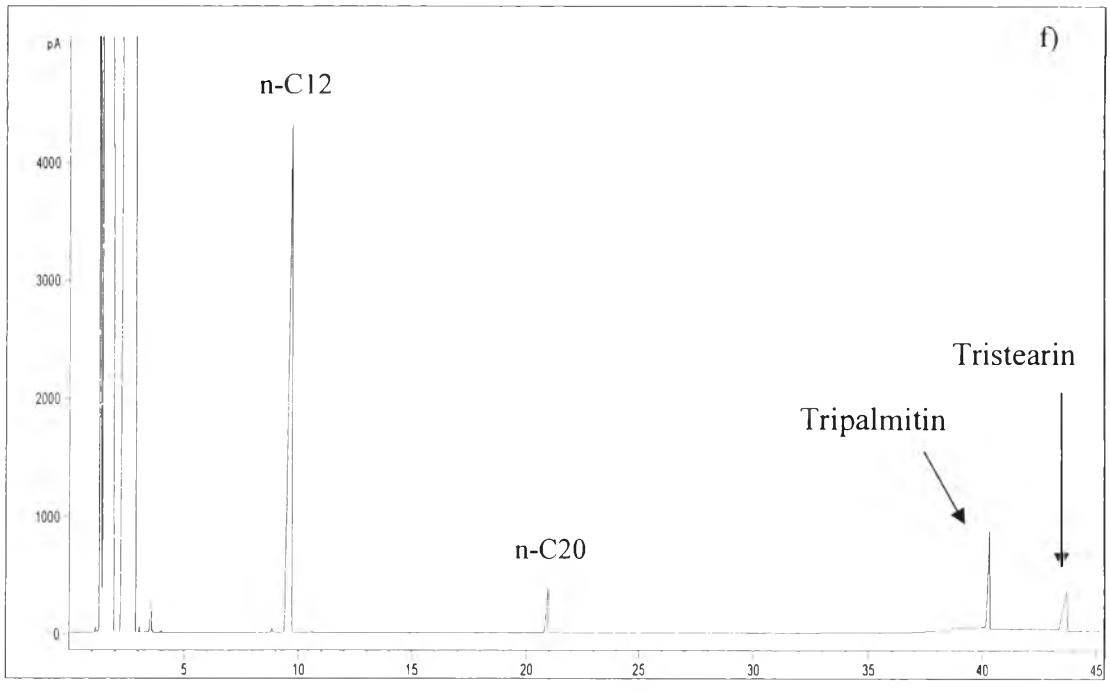

Figure 4.2 (cont.) Chromatograms of standard chemicals, (a) n-pentadecane, n-hexadecane, n-heptadecane, n-octadecane, (b) hexadecanol, octadecanol, palmitic acid, stearic acid, oleic acid, (c) monopalmitin, (d) stearyl palmitate, palmityl stearate, stearyl stearate, (e) dipalmitin, distearin, and (f) tripalmitin, tristearin.

Table 4.2 Retention times and response factors of standard chemicals

Standard chemicals	Retention times	Response factors
n-Pentadecane	14.208	1.034
n-Hexadecane	15.506	1.029
n-Heptadecane	16.679	1.029
n-Octadecane	17.904	1.047
Hexadecanol	20.707	1.092
Octadecanol	27.293	1.078
Palmitic acid	22.878	1.103
Stearic acid	29.082	1.045
Oleic acid	28.600	0.985
Stearyl palmitate	35.562	1.077
Palmityl stearate		0.912
Stearyl stearate	36.132	0.975
Monopalmitin	32.835	1.103
Dipalmitin	36.559	0.972
Distearin	37.558	0.971
Tripalmitin	40.326	0.989
Tristearin	43.685	0.946

4.2.2 Feed Analysis

The 30 vol.% fats and oils (beef fat, chicken fat, pork fat, jatropha oil, and palm oil) in dodecane were analyzed with gas chromatograph to identify their components. The result shows that all feestocks contain triglyceride as main component except in palm oil which also has high amount of monoglycerides, diglycerides and palmitic acid. In all feedstocks, trace amount of free fatty acid e.g. oleic acid and stearic acid were observed. The GC chromatograms and composition of all feedstocks are shown in Figure 4.3 and Table 4.3. respectively.

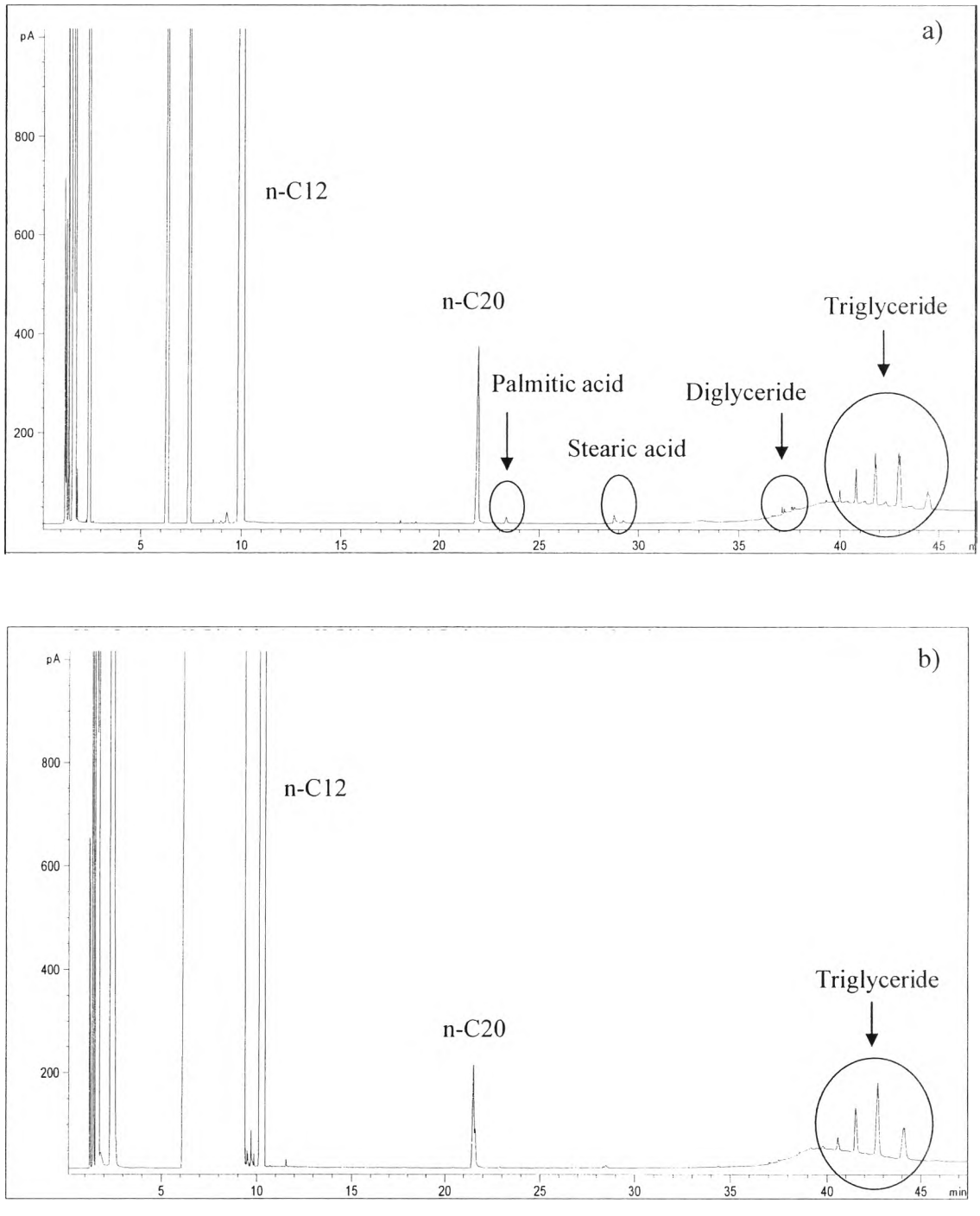

Figure 4.3 Chromatograms of 30 vol.% triglyceride-based feedstocks in dodecane, (a) beef fat, (b) chicken fat, (c) pork fat, (d) jatropha oil, and (e) palm oil.

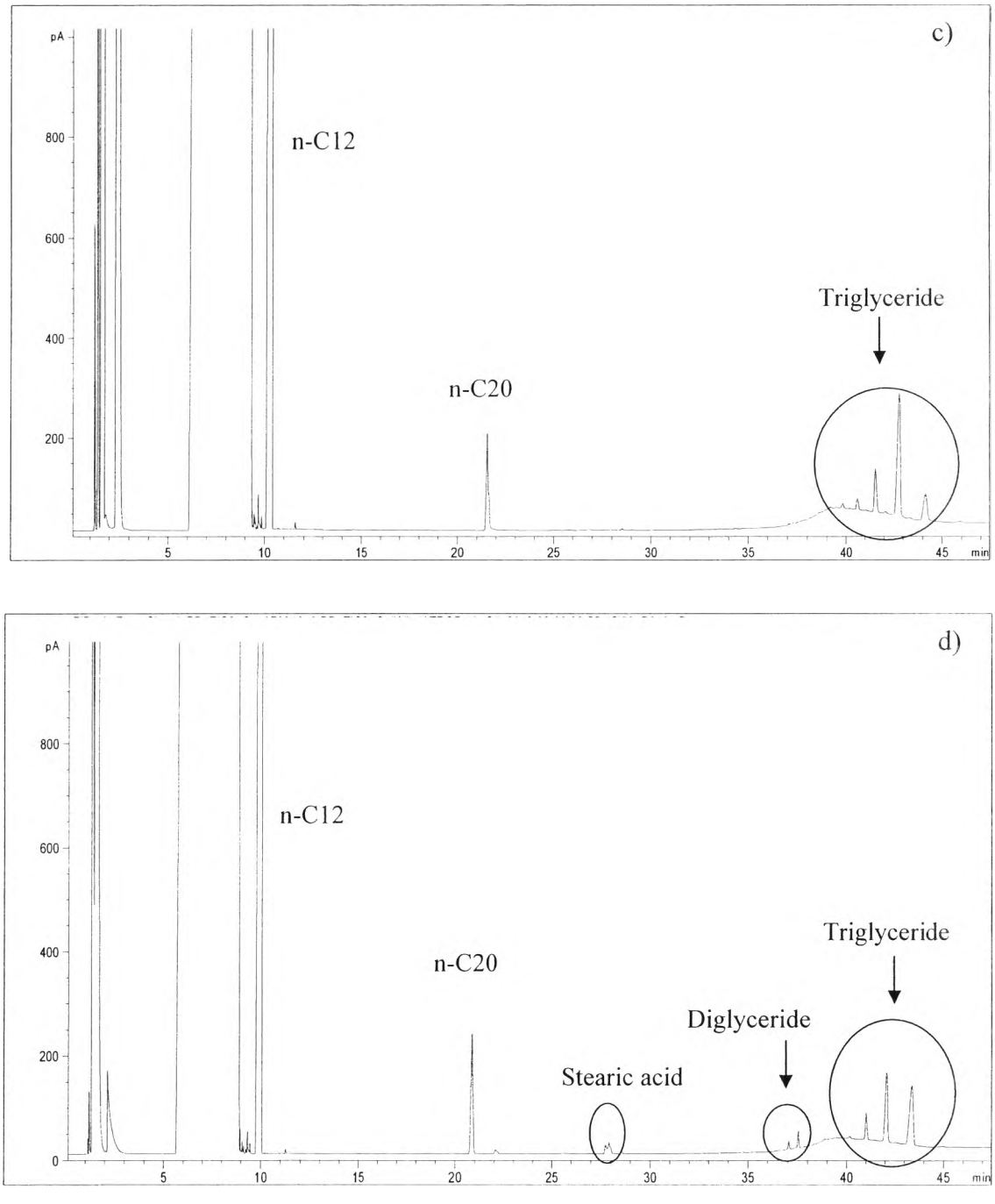

Figure 4.3 (cont.) Chromatograms of 30 vol.% triglyceride-based feedstocks in dodecane, (a) beef fat, (b) chicken fat, (c) pork fat, (d) jatropha oil, and (e) palm oil.

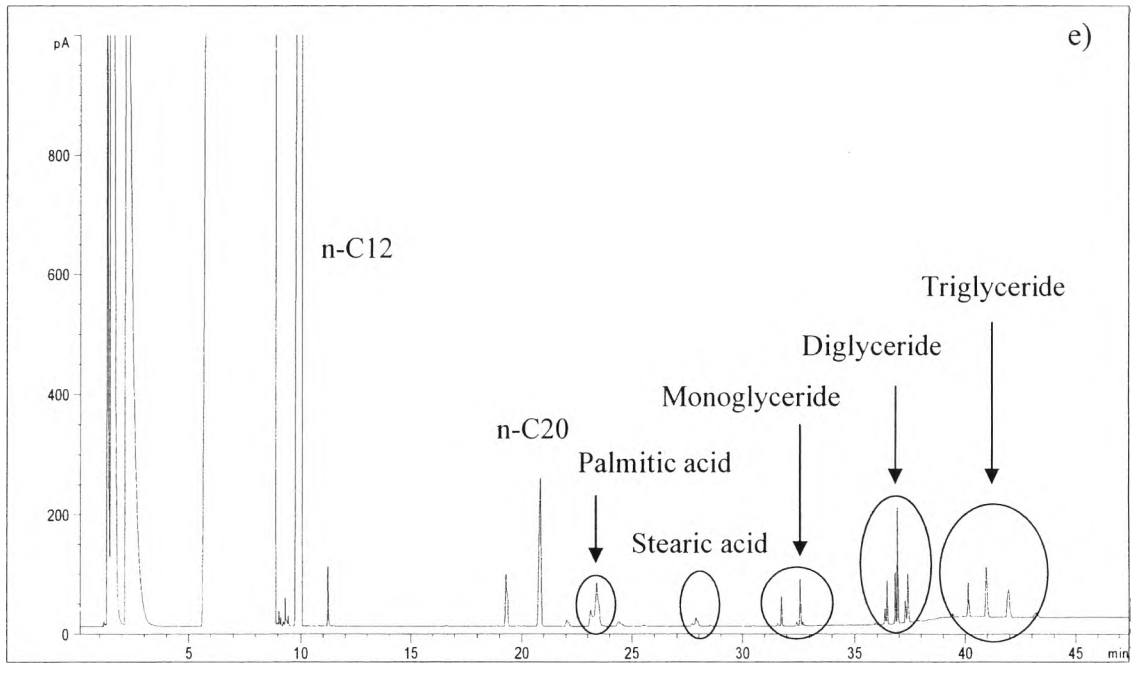

Figure 4.3 (cont.) Chromatograms of 30 vol.% triglyceride-based feedstocks in dodecane, (a) beef fat, (b) chicken fat, (c) pork fat, (d) jatropha oil, and (e) palm oil.

Table 4.3 Composition of triglyceride based feedstock from gas chromatography

Composition	Beef Fat (wt.%)	Chicken fat (wt.%)	Pork fat (wt.%)	Jatropha oil (wt.%)	Palm oil (wt.%)
Triglycerides	79.84	98.76	99.79	81.79	23.57
Diglycerides	10.60	-	-	6.69	29.48
Monoglycerides	-	-		-	7.78
Oleic acid	5.13	1.24	0.21	0.80	-
Palmitic acid	2.84	-	-	2.13	24.70
Stearic acid	1.59	-	-	8.59	2.94
Unknown	-	-	-	-	11.53

From Table 4.3, the peak at retention time approximately 19 in palm oil feedstock was also observed. This composition might occur during the storage.

Table 4.4 Fatty acid compositions of feedstocks investigated in this work

Fatty Acid	Systematic name	Acronym	Formular	M.W.	Composition (wt.%)				
					Palm oil	Jatropha oil	Beef fat	Pork fat	Chicken fat
Caprylic acid	Octanoic acid	8:0	$C_8H_{16}O_2$	144.22	0.02	-	0.02	-	-
Capric acid	Decanoic acid	10:0	$C_{10}H_{20}O_2$	172.27	0.02	-	0.05	0.09	0.01
Lauric acid	Dodecanoic acid	12:0	$C_{12}H_{24}O_2$	200.32	0.22	-	0.11	0.33	0.03
Myristic acid	Tetradecanoic acid	14:0	$C_{14}H_{28}O_2$	228.38	1.01	0.06	3.30	1.84	0.49
	Pentadecanoic acid	15:0	$C_{15}H_{30}O_2$	242.4	0.05	0.02	0.39	0.05	0.06
Palmitic acid	Hexadecanoic acid	16:0	$C_{16}H_{32}O_2$	256.43	40.06	13.81	26.13	21.44	20.08
	Heptadecanoic acid	17:0	$C_{17}H_{34}O_2$	270.45	0.10	0.10	0.67	0.27	0.10
Stearic acid	Octadecanoic acid	18:0	$C_{18}H_{36}O_2$	284.48	4.39	6.89	16.38	9.40	4.34
Arachidic acid		20:0	$C_{20}H_{40}O_2$	312.53	0.34	0.22	0.15	0.14	0.09
Behenic acid		22:0	$C_{22}H_{44}O_2$	340.59	0.06	0.04	-	-	0.02
Lignoceric acid		24:0	$C_{24}H_{48}O_2$	368.64	0.07	0.05	-	-	0.02
Palmitoleic acid		16:1	$C_{16}H_{30}O_2$	254.41	0.18	0.79	0.84	1.96	3.45
cis-9-Oleic acid	cis-9-Octadecenoic acid	18:1	$C_{18}H_{34}O_2$	282.47	40.72	45.84	40.71	39.23	33.78
cis-11-Eicosenoic acid		20:1	$C_{20}H_{38}O_2$	310.52	0.14	0.08	0.88	0.75	0.28
Erucic acid		22:1	$C_{22}H_{42}O_2$	338.58	-	-	-	0.16	0.02
Linoleic acid	Octadecadienoic acid	18:2	$C_{18}H_{32}O_2$	280.45	12.08	31.77	1.18	17.10	29.16
α-Linolenic acid	Octadecatrienoic acid	18:3	$C_{18}H_{30}O_2$	278.44	0.38	0.21	0.08	1.40	2.37
cis-11,14-Eicosadienoic acid		20:2	$C_{20}H_{36}O_2$	308.5	0.02	0.02	-	0.55	0.16
cis-11,14,17-Eicosadienoic acid		20:3	$C_{20}H_{34}O_2$	306.49	-	-	0.11	0.32	0.02

The fatty acid compositions of all feedstocks were also analyzed followed the AOAC 996.06-GC method. From Table 4.4, the main fatty acids in all feedstocks are palmitic acid ($C_{16}H_{32}O_2$) and oleic acid ($C_{18}H_{34}O_2$).

4.2.3 Inductively Coupled Plasma Optical Emission Spectrometry (ICP-OES)

The inductively coupled plasma optical emission spectrometry was used to detect the amount of trace elements which are the main impurities in feedstocks. The metals investigated in this work are Mg, Na, P, Ca, and K. The amount of metals in each feedstocks are shown in Table 4.5. From the result, all feedstocks contain the significant concentrations of impurities.

Table 4.5 Concentration of main impurities in each feedstocks

Feed	Mg (ppm)	Na (ppm)	K (ppm)	Ca (ppm)	P (ppm)	M eq. (mmol/kg)	P (mmol/kg)
Beef fat	2.14	54.20	7.03	25.01	16.61	1.98	0.54
Chicken fat	1.63	5.70	2.32	14.06	8.31	0.57	0.27
Pork fat	1.84	5.14	2.16	14.68	10.01	0.58	0.32
Jatropha oil	3.62	4.43	1.98	19.44	20.28	0.76	0.65
Palm oil	8.60	70.09	238.05	12.87	6.52	5.26	0.21

The impurities were classified into two groups, alkali (Mg, Na, K, and Ca) and phosphorus. Alkalis are the natural impurities in feedstock and phosphorus is the representation of phospholipids. From Table 4.5, palm oil shows the highest concentration of impurities followed by beef fat, jatropha oil, pork fat, and chicken fat, respectively.

4.3 Catalytic Activity Testing

4.3.1 Product Analysis

To study the catalytic activity and selectivity in deoxygention over Pd/TiO_2 catalyst, the production of hydrogenated biodiesel from beef fat, chicken fat, pork fat, jatropha oil, and palm oil were conducted at 325 ^{o}C, 500 psig, liquid hourly space velocity (LHSV) of 4 h^{-1}, and H_2/feed molar ratio of 30 for 6 h. The liquid product was analyzed by gas chromatograph. Table 4.6 summarizes the conversions and the product selectivity of all feedstocks at various times on stream.

The results showed that all triglyceride-based feedstocks can be converted to long chain hydrocarbons in diesel specification range (C15-C18). The main products obtained from all feedstocks were n-pentadecane (n-C15) and n-heptadecane (n-C17), resulting from the decarbonylation/decarboxylation reaction which one carbon atom is removed out of original fatty acids in each oil molecule (Huber *et al.*, 2007 and Snare *et al.*, 2006). The intermediates such as stearic acid, oleic acid, palmitic acid and the others products like tridecane (C13) and tetradecane (C14) are also detected.

Figure 4.4 summarizes the conversion and the selectivity of C15-C18 at various times on stream.

Table 4.6 Conversion and product selectivity from hydrodeoxygenation over Pd/ TiO_2 catalyst (Reaction conditions: T = 325 °C, P = 500 psig, H_2/feed molar ratio of 30, and LHSV = 4 h^{-1})

Feedstock	Beef fat			Pork fat			Chicken fat			Jatropha oil			Palm oil		
Time on stream (h)	2	4	6	2	4	6	2	4	6	2	4	6	2	4	6
Conversion	40.61	33.70	24.24	56.27	50.08	46.21	51.81	41.32	37.85	61.97	56.41	56.77	40.96	24.89	14.87
Selectivity (%)															
Total C15-C18	56.18	50.50	52.59	59.61	54.98	52.46	58.61	51.75	47.70	52.80	49.79	49.23	42.42	21.05	19.31
n-C15	14.08	11.17	12.53	14.19	12.98	12.20	14.94	13.22	12.37	8.25	7.48	7.33	13.09	7.46	6.80
n-C16	4.67	5.31	4.69	2.61	2.50	2.54	2.16	1.86	1.57	1.12	1.29	1.44	2.40	0.83	0.73
n-C17	29.55	24.45	27.05	37.34	34.29	32.41	37.01	32.77	30.53	39.44	36.30	35.19	23.49	11.67	10.83
n-C18	7.87	9.56	8.32	5.47	5.21	5.31	4.49	3.89	3.24	4.00	4.72	5.27	3.45	1.09	0.95
$\frac{(C15+C17)}{(C16+C18)}$	3.48	2.39	3.04	6.38	6.13	5.68	7.80	7.99	8.92	9.32	7.29	6.33	6.26	9.95	10.50
Intermediates	39.25	45.05	42.88	38.59	43.25	45.75	40.08	47.08	51.14	46.62	49.64	50.18	50.91	62.78	64.19
hexadecanol	0.00	0.00	0.00	1.17	1.10	1.06	0.65	0.65	0.52	0.00	0.00	0.00	1.48	8.33	6.49
palmitic acid	6.80	7.70	7.22	4.35	4.76	5.14	5.57	6.97	7.96	3.74	3.67	3.71	6.51	7.73	8.60
oleic acid	2.47	2.51	2.65	11.94	13.26	13.72	13.39	15.93	17.73	17.54	16.25	16.52	11.62	11.93	12.71
stearic acid	15.10	16.59	16.22	1.84	2.18	2.30	1.64	2.81	3.18	2.05	3.25	3.53	2.17	2.37	2.50
Esters	12.50	14.65	13.90	17.43	19.86	21.92	16.82	17.87	18.84	23.29	26.47	25.60	0.00	0.00	0.00
diglycerides	2.38	3.60	2.90	1.85	2.09	1.62	2.01	2.86	2.91	0.00	0.00	0.82	8.81	14.81	33.90
Others	4.57	4.45	4.53	1.90	1.79	1.59	1.31	1.17	1.16	0.58	0.57	0.58	6.67	16.17	16.49

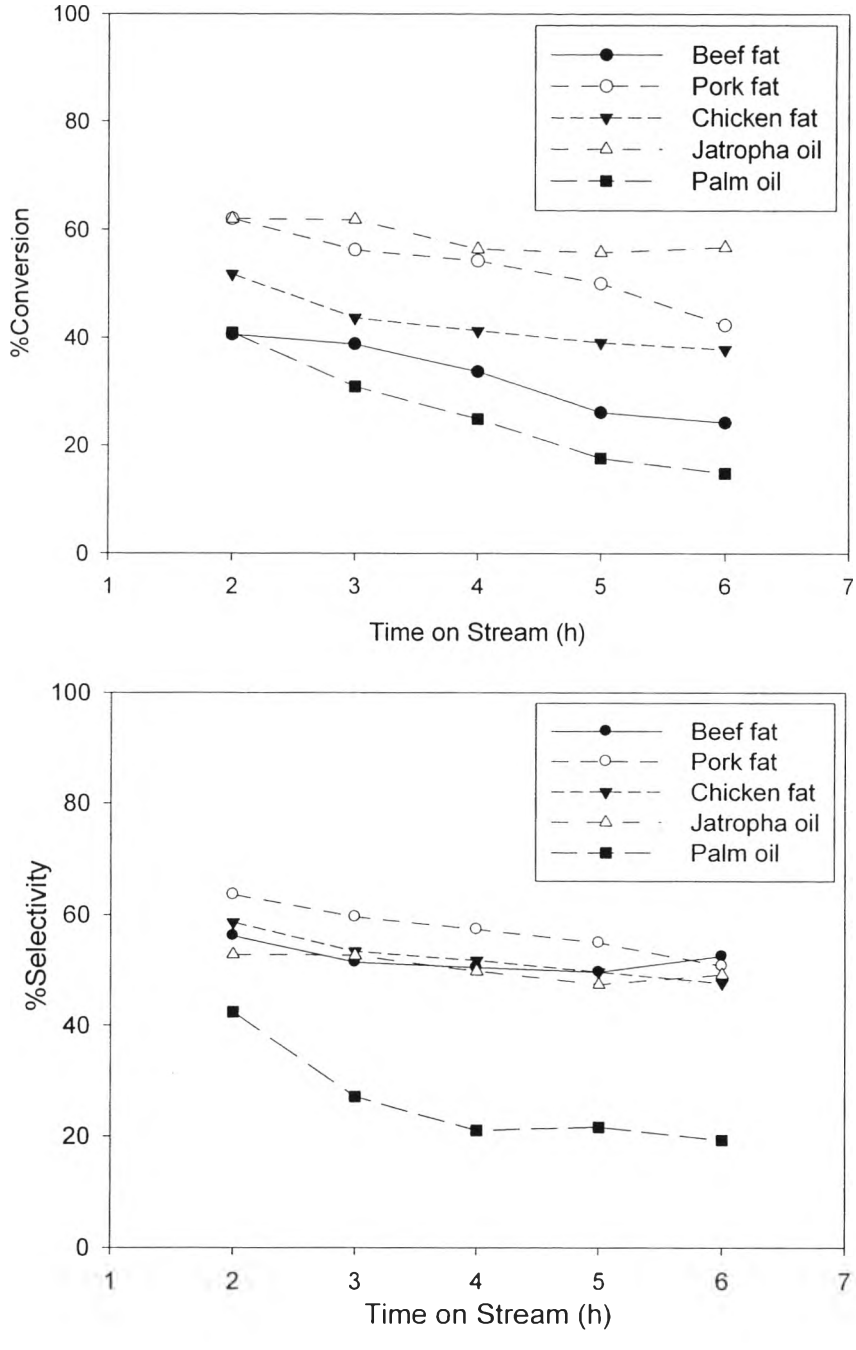

Figure 4.4 Conversion and selectivity of diesel range hydrocarbons (C15-C18) over Pd/TiO_2 catalyst obtained from various triglyceride based feedstocks. (Reaction condition: P = 500 psig, T = 325 °C, LHSV = 4 h^{-1}, and H_2/feed molar ratio of 30).

From the results, jatropha oil feedstock tends to give the highest conversion followed by chicken fat, pork fat, beef fat, and palm oil, respectively. The conversions of all feedstocks decrease with times which the highest reduction rate was observed in palm oil. The results were not in line with the ICP results, the higher concentration of impurities should give the lower conversion.

Therefore, the balance between the cations (alkali) and anions represented by the phosphate anion originating from phospholipids was also studied. Milliequivalent was used to calculate the concentration of cation and anion. However, phosphorous is usually referred to in terms of mmol. Their balance can be seen from the compensation between milliequivalent of alkali cations (M eq.) and concentration of phosphorus (mmol/kg) as shown in Table 4.5. Milliequivalent can be obtained from equation (1), where anion charge was equal to −2, as the phosphate group is bound to the glycerol backbone in phospholipids.

$$\text{M eq.} = \frac{\sum(\text{cation} \cdot \text{charge} \times \text{cation} \cdot \text{conc.})/\text{cation} \cdot \text{atomic} \cdot \text{weight}}{|\text{anion} \cdot \text{charge}|} \qquad (1)$$

In case when the concentration of alkalis cations and phosphate anion are in balance, deposits of alkalis phosphates will be formed that will cause plugging of the reactor. In the case of imbalance between cations and anions or the excess impurities from balance, the deactivation rate will increase with the increasing concentration of impurities (Kubicka, D.. and Horacek, J., 2011).

The most pronounced imbalance was observed for palm oil followed by beef fat, pork fat, chicken fat, and jatropha oil, respectively. This result complied with the catalytic activity result (Figure 4.4), the most imbalance between alkali cation and phosphate anion showed the worst performance. The selectivity toward the product in diesel range hydrocarbons (C15-C18) was not significantly difference for all feedstocks excepted in palm oil which has lower selectivity of C15-C18 and rapidly decline with times. These results may caused by the deposition of metal impurities in each feedstocks on the catalyst surface.

4.4 Spent Catalyst Characterizations

4.4.1 Inductively Coupled Plasma Optical Emission Spectrometry (ICP-OES)

Inductively coupled plasma optical emission spectrometry was used to identify the quantity of active metal on catalyst. The result shows that the actual amount of Pd loaded on TiO_2 support is 0.96%. The result reveals that the technique used in catalyst preparation (incipient wetness impregnation, IWI) gives desired amount in Pd loading on TiO_2 support.

The impurities contents and metal loading on the spent catalysts after reaction of all feedstocks were also investigated by ICP-OES. From Table 4.7, most of impurities contents deposit on the spent catalysts which may reduce the activity of the catalyst. The sintering of metal loading may occur, result in the reduction of Pd content on spent catalyst which can also reduce the catalyst activities.

Table 4.7 Concentration of main impurities and metal loading on spent catalysts after 6 TOS

Fat/oil	Mg (ppm)	Na (ppm)	K (ppm)	Ca (ppm)	P (ppm)	Pd (wt%)
Beef	108.69	760.84	225.59	463.48	184.57	0.81
Chicken	99.44	707.32	230.77	439.02	168.86	0.76
Pork	126.42	616.98	330.19	392.45	235.85	0.88
Jatropha	138.52	508.54	102.47	423.15	199.24	0.78
Palm	135.31	1,894.29	2,780.13	1,050.74	>943.40	0.77

Moreover, the amount of coke deposition on spent catalyst may affected by the concentration of phosphorus (Kubicka, D., and Horacek, J., 2011). Temperature programmed oxidation was also used to estimate the amount of carbon deposition on the spent catalyst after 6 TOS.

4.4.2 Temperature Programmed Oxidation (TPO)

The TPO profiles from temperature programmed oxidation and the amounts of coke deposit on spent catalysts (after 6 TOS) are illustrated in Figure 4.5 and Table 4.8, respectively. For all feedstocks, the peak of coke deposit on the spent catalyst observed at temperature about 350 °C which indicated to the weakly coke.

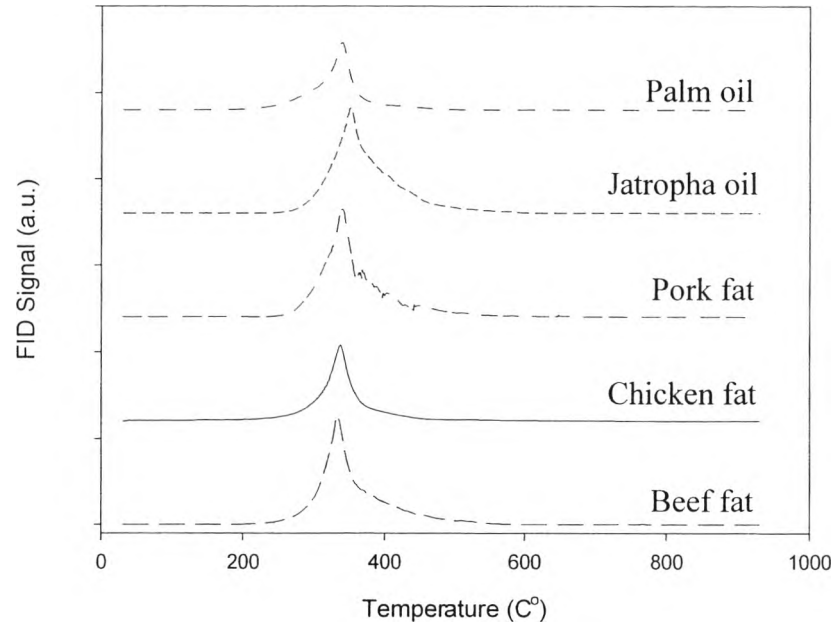

Figure 4.5 TPO profiles of spent catalysts.

Table 4.8 Amount of carbon deposit on the spent catalyst after reaction

Feedstock	Carbon deposit (wt.%)
Beef fat	10.42
Chicken fat	6.26
Pork fat	8.69
Jatropha oil	10.47
Palm oil	6.19

The amount of carbon deposit on the spent catalyst after reaction of jatropha oil is the highest followed by beef fat, pork fat, chicken fat, and palm oil, respectively. Normally, the higher conversion of feedstock should give the lower amount of carbon deposition on the spent catalyst. Jatropha oil which exhibited the highest conversion, showed the highest amount of carbon deposition. This may result from the phosphorus content in feedstock (Table 4.5). The phosphorus in feedstock is representation of phospholipids which can decompose and release phosphoric acid which acts as an oligomerization/polymerization catalyst (Kubicka, D., and Horacek, J., 2011). Palm oil which gave the worst performance also showed the lowest carbon deposition. This result may caused by the deposition of metal on the catalyst surface due to high concentration of alkalis, leading to the blockage or poisoning of active sites.